Journal of Physiology - Paris 103 (2009) 73–87

Contents lists available at ScienceDirect

Journal of Physiology - Paris

journal homepage: www.elsevier.com/locate/jphysparis

# Motif distribution, dynamical properties, and computational performance of two data-based cortical microcircuit templates ☆

Stefan Haeusler *, Klaus Schuch, Wolfgang Maass

*Institute for Theoretical Computer Science, Graz University of Technology, A-8010 Graz, Austria*

ARTICLE INFO

*Keywords:*
Cortical layers
Lamination
Microcircuit Models
Real-Time Computations
Network Motifs
Circuit dynamics

ABSTRACT

The neocortex is a continuous sheet composed of rather stereotypical local microcircuits that consist of neurons on several laminae with characteristic synaptic connectivity patterns. An understanding of the structure and computational function of these cortical microcircuits may hold the key for understanding the enormous computational power of the neocortex. Two templates for the structure of laminar cortical microcircuits have recently been published by Thomson et al. and Binzegger et al., both resulting from long-lasting experimental studies (but based on different methods).

We analyze and compare in this article the structure of these two microcircuit templates. In particular, we examine the distribution of network motifs, i.e. of subcircuits consisting of a small number of neurons. The distribution of these building blocks has recently emerged as a method for characterizing similarities and differences among complex networks. We show that the two microcircuit templates have quite different distributions of network motifs, although they both have a characteristic small-world property. In order to understand the dynamical and computational properties of these two microcircuit templates, we have generated computer models of them, consisting of Hodgkin–Huxley point neurons with conductance based synapses that have a biologically realistic short-term plasticity. The performance of these two cortical microcircuit models was studied for seven generic computational tasks that require accumulation and merging of information contained in two afferent spike inputs. Although the two models exhibit a different performance for some of these tasks, their average computational performance is very similar. When we changed the connectivity structure of these two microcircuit models in order to see which aspects of it are essential for computational performance, we found that the distribution of degrees of nodes is a common key factor for their computational performance. We also show that their computational performance is correlated with specific statistical properties of the circuit dynamics that is induced by a particular distribution of degrees of nodes.



## 1. Introduction

Many complex networks from biochemistry and neurobiology as well as engineering share certain global properties (Newman, 2003; Strogatz, 2001; Watts and Strogatz, 1998), like degree distributions (distribution of the number of edges per node) and small-world properties, i.e. local clustering of edges in a graph while maintaining a short path between nodes. But they often have different local properties, yielding different distributions of stereotypical connectivity patterns for few nodes, called motifs (Milo et al., 2002, 2004; Shen-Orr et al., 2002).

Neurobiological studies have shown that cortical circuits have a distinctive modular and laminar structure, with stereotypical connections between neurons that are repeated throughout many cortical areas (Douglas et al., 1995; Douglas and Martin, 2004; Kalisman et al., 2005; Mountcastle, 1998; Nelson, 2002; Silberberg et al., 2002; White, 1989). It has been conjectured that these stereotypical canonical microcircuits are not merely an artifact of the specific mapping of afferent and efferent cortical pathways or other anatomical constraints like evolutionary processes or development, but are also advantageous for generic computational operations that are carried out throughout the neocortex.

Over the past years detailed statistical data became available that are based on two different experimental methods: dual intracellular recordings in vitro and cell morphology. The first dataset assembled by Thomson et al. (2002) was estimated from 998

☆ Written under partial support by the Austrian Science Fund FWF # S9102-N13 and project # FP6-015879(FACETS), project # FP7-216593 (SECO), project # FP7-506778 (PASCAL2) as well as project # FP7-231267 (ORGANIC) of the European Union.

* Corresponding author.
*E-mail addresses:* haeusler@igi.tugraz.at (S. Haeusler), schuch@igi.tugraz.at (K. Schuch), maass@igi.tugraz.at (W. Maass).

0928-4257/$ - see front matter © 2009 Elsevier Ltd. All rights reserved.
doi:10.1016/j.jphysparis.2009.05.006

paired intracellular recordings with sharp electrodes in slices of somatosensory, motor and visual areas of adult rats and adult cats. It specifies connection probabilities and connection strengths of effectively established synaptic connections between excitatory and inhibitory neocortical neurons, to which we will refer as functional connectivity in this paper. The second dataset assembled by Binzegger et al. (2004) was predicted from bouton and target densities in cat primary visual cortex estimated from three-dimensional cell reconstructions. This dataset does not specify the distribution of functional connections, but rather represents potential synaptic connectivity. The probabilities of synaptic connections between excitatory and inhibitory neurons located in different layers, i.e. layer 2/3, 4 and 5, differ significantly for the functional and the potential microcircuit template (see Thomson and Lamy, 2007). In addition this dataset also includes neurons in layer 6.

We investigate these two cortical microcircuit templates with regard to structural and functional properties. In order to evaluate the computational properties of microcircuit templates we carried out computer simulations of detailed cortical microcircuit models consisting of 560 Hodgkin–Huxley type point neurons and synaptic connections with stereotypical dynamic properties (such as paired pulse depression and paired pulse facilitation) from Markram et al. (1998). Similar to Häusler and Maass (2007), our analysis is based on the assumption that stereotypical cortical microcircuits have some "universal" computational capabilities, and can support quite different computations in different cortical areas. Consequently we concentrate on generic information processing capabilities that are likely to be needed for many concrete computational tasks: to accumulate, hold and fuse information contained in Poisson input spike trains from two different sources (modeling thalamic or cortical feedforward input that arrives primarily in layer 4, and lateral or top-down input that arrives primarily in layer 2/3). In addition we examine the capability of such circuit models to carry out linear and nonlinear computations on time-varying firing rates of these two afferent input streams. In order to avoid rather arbitrary assumptions about the specific type of neuronal encoding of the results of such computations, we analyzed how much information is available about the results of such computations to the generic "neural users", i.e., to pyramidal neurons in layer 2/3 (which typically project to higher cortical areas) and to pyramidal neurons in layer 5 (which typically project to lower cortical areas or to subcortical structures, but also project for example from V1 back to nonspecific thalamus, i.e. to the intralaminar and midline nuclei that do not receive direct primary sensory input, and through this relay to higher cortical areas, see Callaway (2004)).

In Häusler and Maass (2007) it was shown that the cortical microcircuit model based on the template from Thomson et al. (2002) exhibits specific computational advantages over various types of control circuits that have the same components and the same global statistics of neurons and synaptic connections, but are missing the lamina-specific structure of real cortical microcircuits. Furthermore it was demonstrated that the connectivity graphs defined by this cortical microcircuit template has a small-world property. However we had shown that the degree distribution of neurons is more salient for their computational performance than the small world property.

Here we extend this study by showing that the two cortical microcircuit templates of Thomson et al. (2002) and Binzegger et al. (2004) share some global structural properties, like degree distributions and small-world properties, but have significantly different local structural properties, i.e. network motif distributions. A comparison of the information processing capabilities of both microcircuit templates reveals that they have a similar average computational performance but significantly different computational properties for specific tasks. We also address the question which aspect of the microcircuit template of Binzegger et al. (2004) is essential for its computational performance, by scrambling specific aspects of their connectivity pattern in a variety of control circuits. We find that, like for the template of Thomson et al. (2002), the degree distribution of nodes is essential for its computational performance. This result is, besides their similar average computational performance, a second common property of these otherwise quite dissimilar microcircuit templates. We also identify specific properties of the dynamics of the two networks that correlate with their superior computational performance.

## 2. Methods

### 2.1. Microcircuits and computational tasks

We analyzed cortical microcircuit models based on the laminae-specific connectivity pattern specified by two different cortical microcircuit templates. The first cortical microcircuit template assembled by Thomson et al. (2002) was estimated from paired intracellular recordings with sharp electrodes from 998 pairs of identified neurons from somatosensory, motor and visual areas of adult rats, and visual areas of adult cats. The sampling was made randomly within a lateral spread of 50—100 μm (Thomson, 2005). This cortical microcircuit template specifies functional synaptic connectivity, i.e. connection probabilities and efficacies of synaptic connections between neurons located in six different populations (excitatory and inhibitory neurons in layers 2/3, 4, 5). For those pairs where both data from rat and from cat are given in Thomson et al. (2002), we have taken the data from rat (see Fig. 1). Only for pairs of neurons within layer 4 no data from rat are given in Thomson et al. (2002), hence the corresponding data are from cat.[1] We analyzed a model of this microcircuit template that consisted of 560 neurons, with 30%, 20%, and 50% of the neurons assigned to layer 2/3, layer 4, and layer 5, respectively (the number 560 was chosen somewhat arbitrarily, based on required simulation speed and programming details). We will refer to the microcircuit model based on this cortical microcircuit template as Thomson et al. circuit.[2]

The second cortical microcircuit template assembled by Binzegger et al. (2004) was predicted from bouton and target densities in cat primary visual cortex estimated from three-dimensional reconstructions of cells in vivo. This cortical microcircuit template specifies potential synaptic connectivity between neurons located in 10 specific populations (excitatory and inhibitory neurons in layers 1, 2/3, 4, 5 and 6). We omitted layer 1, because it only receives input and provides no synaptic connections back to other layers, and is therefore irrelevant for the analysis in this study. The connectivity graph of the eight modeled populations is shown in Fig. 2. A number of additional unassigned connections were reported in Binzegger et al. (2004). These were not considered for the calculation of connection probabilities in this article. The synaptic connection probabilities were further rescaled to achieve on average the same number of 42,540 synaptic connections as obtained for the Thomson et al. circuits. This resulted in a mean connection probability of 13% or, equivalently, an average number of 76 recurrent synaptic connections per neuron. The microcircuit model consisted of 560 neurons, with 36%, 36%, 7% and 21% of the neurons assigned to layer 2/3, layer 4, layer 5 and layer 6, respectively (see Binzegger

[1] Some of the pairings were rarely observed and the corresponding entries suffer from small sample size (see Thomson et al., 2002 for details). Also very small neurons in rat may have been missed in this study (Thomson, 2005). In addition it is likely that in some cortical microcircuits connections exist between pairs of neurons for which no connections were reported in Thomson et al. (2002) (see for example (Dantzker and Callaway, 2000) for the case of connections to inhibitory neurons in layers 2/3).

[2] One should note that the layers defined by this and other microcircuit templates are not induced by their graph structure (like the layers in a multi layer perceptron). Rather the layer to which a neuron belongs should formally be viewed as a label of the corresponding node in the graph.

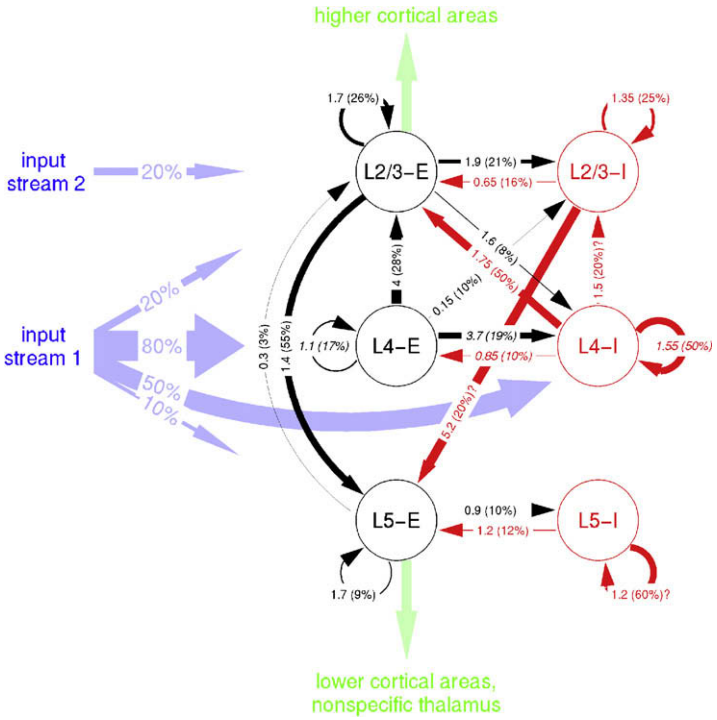


**Fig. 1.** Cortical microcircuit template estimated from paired intracellular recordings according to Thomson et al. (2002). Numbers at arrows denote connection strengths (mean amplitude of postsynaptic potentials, PSPs, measured at soma in mV) and connection probabilities (in parentheses), for connections between cortical neurons in three different layers, each consisting of an excitatory (E) and an inhibitory (I) population, with an estimated maximal horizontal distance of up to 100 μm. The width of arrows is proportional to the product of these two numbers. Most of the data are from rat cortex, except for interconnections in layer 4 (italic), which are from cat. Input stream 1 models feedforward inputs, and input stream 2 models top-down or lateral input to the cortical microcircuit. Percentages at input streams denote connection probabilities for input neurons (that produce these input streams) in our simulations. Figure reproduced with permission of Häusler and Maass (2007).

et al. (2004) for a discussion of data which justify these estimates).[3] Because the cortical microcircuit template of Binzegger et al. (2004) provides no strengths of synaptic connections (i.e., synaptic weights), we modeled the distribution of synaptic weights according to the cortical microcircuit template of Thomson et al. (2002). The strengths of synaptic connections from and to layer 6, which do not occur in Thomson et al. circuits, were set to the average values of all other connections of the corresponding synapse type.[4] These weights are labeled with "?" in Fig. 2. We will refer to microcircuit models based on the second cortical microcircuit template as Binzegger et al. circuits. Each layer of both cortical microcircuit templates consisted of a population of excitatory neurons and a population of inhibitory neurons with a ratio of 4:1.

The short term dynamics of cortical synapses (i.e., their specific mixture of paired pulse depression and paired pulse facilitation) is known to depend on the type of the presynaptic and postsynaptic neuron. We modeled the short term synaptic dynamics according to the model proposed in Markram et al. (1998), with synaptic parameters chosen as in Maass et al. (2002) to fit data from microcircuits in rat somatosensory cortex (based on Gupta et al., 2000; Markram et al., 1998). The maximum conductances of synapses were chosen from a Gaussian distribution with a SD of 70% of its mean (the negative values were replaced by values chosen from an uniform distribution between zero and two times the mean).[5] The mean maximum conductances of synapses were chosen to reproduce the mean amplitude of PSPs given in Figs. 1 and 2 at the resting membrane potential (in the presence of synaptic background activity). Synaptic transmission delays between neurons were chosen from Gaussian distributions with mean 1.5 ms (0.8 ms) for connections between excitatory neurons (all other connections) and a standard deviation of 0.1 times the mean.

Excitatory and inhibitory neurons were modeled as conductance based single compartment Hodgkin–Huxley neuron models with passive and active properties modeled according to Destexhe et al. (2001). A cortical neuron receives synaptic inputs not only from immediately adjacent neurons, but also smaller background input currents from a large number of more distal neurons, causing in awake animals a depolarization of the membrane potential commonly referred to as 'high conductance state'. This was reflected in our computer model by background input currents that were injected into each neuron. The conductances of these background currents were modeled as a one-variable stochastic process similar to an Ornstein–Uhlenbeck process with parameters obtained from a biophysical model matched to intracellular recordings from a L5 neuron from cat cerebral cortex Destexhe et al. (2001).

Two afferent input streams, each consisting of 4 or 40 spike trains (i.e., 4 or 40 input channels), were injected into the circuit. Each of the channels of the first input stream (representing thalamic, or feedforward cortical input) was injected mainly into layer 4, i.e. to 50% of its inhibitory neurons and 80% of its excitatory neurons, but also into 20% of the excitatory neurons in layer 2/3 and 10% of the excitatory neurons in layer 5 (all randomly chosen). Each of the channels of the second afferent input stream was injected into 20% of the excitatory neurons in layer 2/3. The mean maximum conductances of all input synapses were chosen to generate a PSP with a mean amplitude of 1.9 mV at the resting membrane potential in the presence of background input. Input synapses were chosen to be static and their maximum conduc-

[3] We verified that the reported results are qualitatively the same for circuits consisting of up to 1000 neurons. In general, the performance scales with the network size (see Häusler and Maass, 2007).

[4] Synapse types are defined according to the post-and presynaptic neuron type.

[5] No observable differences occurred in case of replacing this distribution with a gamma distribution with a scale parameter that equals the specified mean and a shape parameter of 1.

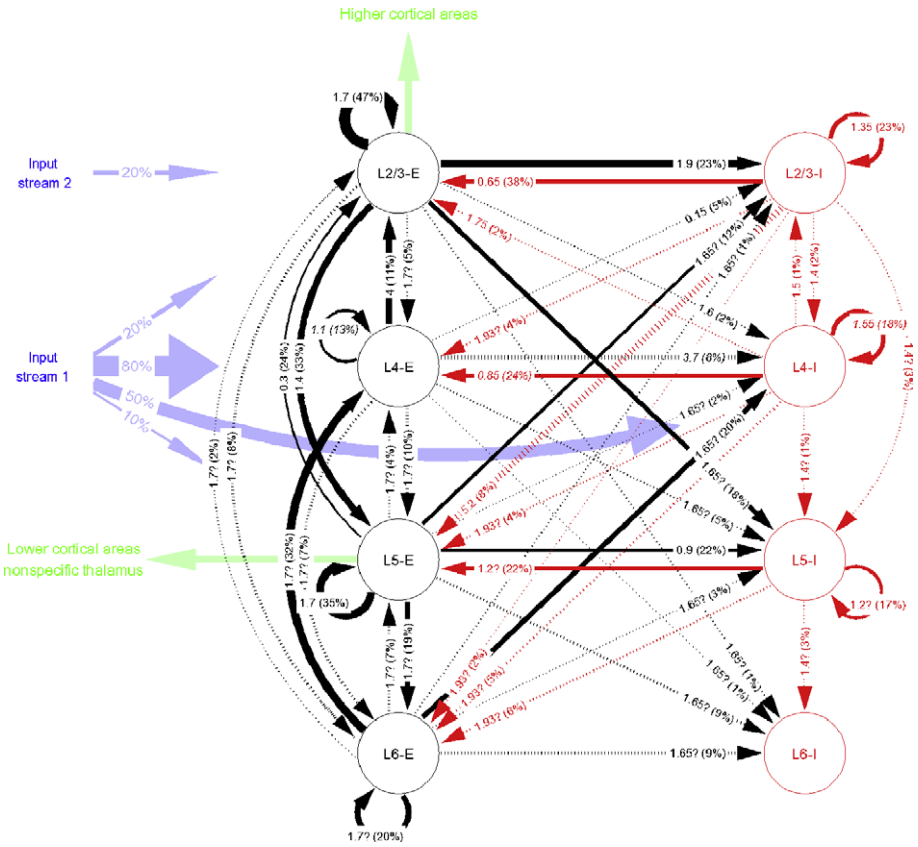


**Fig. 2.** Cortical microcircuit template predicted from bouton and target densities estimated from three-dimensional cell reconstructions according to Binzegger et al. (2004). Numbers at arrows denote connection strengths (mean amplitude of postsynaptic potentials, PSPs, measured at soma in mV) and connection probabilities (in parentheses), for connections between cortical neurons in four different layers, each consisting of an excitatory (E) and an inhibitory (I) population. Connection probabilities were estimated from 39 three-dimensional single neuron reconstructions from cat primary visual cortex. Connection strengths were taken from the cortical microcircuit template described in Thomson et al. (2002) (see Fig. 1). Weights with question marks denote unspecified connections (see text). Dashed lines denote connections that were pruned for the experiments described in Section 3.1. The length of dashes and the width of solid lines indicate the product of the probability and the strength of a synaptic connection.

tances were chosen from a Gaussian distribution with a SD of 70% of its mean (with negative values replaced by values chosen from an uniform distribution between zero and two times the mean).

In addition to these data there remain three parameters $S_{I1}$, $S_{I2}$ and $S_{RW}$ that scale (in the form of multiplicative factors) the amplitudes of PSPs for all recurrent synapses, and EPSPs from the two input streams (1 and 2). These parameters were adjusted for inputs consisting of 40 Poisson spike trains at 20 Hz to induce biologically plausible average firing rates. The parameter $S_{I1}$ ($S_{I2}$) was chosen so that its respective afferent input stream caused in the absence of the other input stream $S_{I2}$($S_{I1}$) and without recurrent connections ($S_{RW} = 0$) but with background input currents injected into each neuron an average firing rate of 15 Hz in layer 4 (10 Hz in layer 2/3). The parameter $S_{RW}$ was set to a value that produced for the previously fixed parameters $S_{I1}$ and $S_{I2}$ in the presence of synaptic background noise a realistic low but significant firing activity of 8.5 Hz in layer 5 and an average firing rate of 24 Hz in layer 2/3, layer 4 and layer 5. To achieve these firing rates for the Binzegger et al. circuits, the parameter $S_{RW}$ had to be scaled down by a factor of 3.3 compared with its value for the Thomson et al. circuits. For the analysis reported in Figs. 8 and 10 we performed simulations with 40 randomly chosen scaling parameters ($S_{I1}$, $S_{I2}$ and $S_{RW}$) that were drawn uniformly from the interval [0.2, 2] times the previously described standard values. The resulting average firing rates ranged from 4 to 55 Hz.

We further modeled hypothetical projection neurons in layer 2/3 and layer 5. The set of presynaptic neurons for such a hypothetical readout neuron was chosen according to Fig. 1 for Thomson et al. circuits and Fig. 2 for Binzegger et al. circuits, but no synaptic connections from a readout neuron back into the circuit were included. This amounted for the Thomson et al. circuits to an average of 84 presynaptic neurons for a readout neuron in layer 2/3, and 109 presynaptic neurons for a readout neuron on layer 5. To allow a fair comparison between the two cortical microcircuit templates the connections probabilities for the hypothetical readout neurons of Binzegger et al. circuits were rescaled by a multiplicative factor to obtain the same number of presynaptic neurons for each of the two readout neurons.

The projection or readout neurons themselves were modeled as linear neurons, i.e., their output was a weighted sum of low pass filtered spikes (exponential decay with a time constant of 15 ms, modeling the time constants of synaptic receptors and membrane of a readout neuron). The weights of synaptic connections from the presynaptic neurons to the readout neuron were optimized for specific tasks. Care was taken to make sure that weights from excitatory (inhibitory) presynaptic neurons could not become negative (positive) by using a standard method of linear regression with sign-constraints.

The information processing tasks comprised spike pattern classification tasks, i.e. classification of spike patterns in either of the two afferent input streams, memory tasks (classification of earlier spike patterns in one of the two input streams), and non-linear fusion of information from spike patterns in both input streams, as well as real-time computations on the firing rates of both input streams. For information processing tasks with spike patterns we randomly generated spike pattern templates consisting of 30 ms segments of 40 Poisson spike trains at 20 Hz (see Fig. 3). More precisely, the spike trains of each of the two input streams were of length

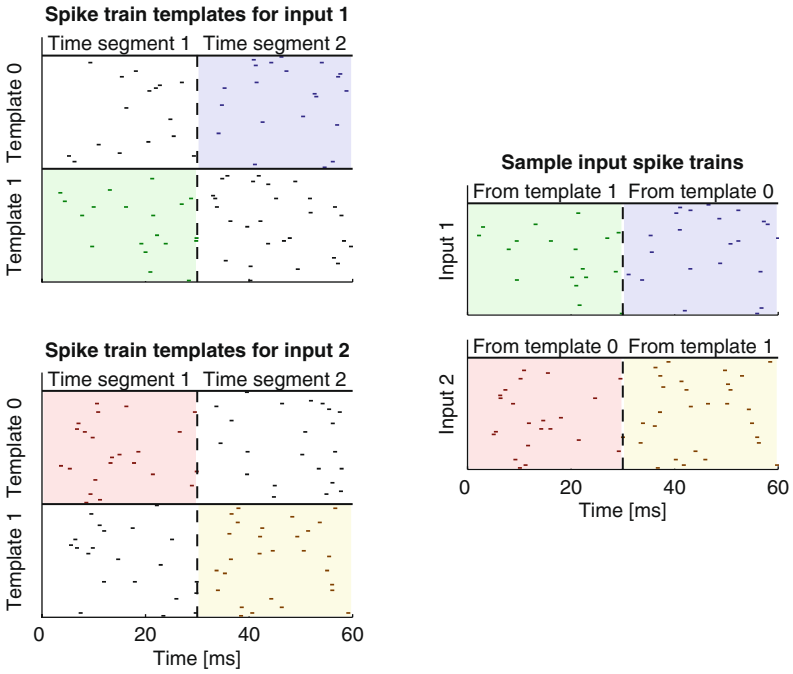


**Fig. 3.** Input distributions for the spike pattern classification/memory and exclusive-or (XOR) tasks. The spike trains of each of the two input streams were of length 450 ms and consisted of 15 time segments of length 30 ms. For each segment two templates were generated randomly (40 Poisson spike trains at 20 Hz). The actual spike trains of each input of length 450 ms used for training or testing were generated by choosing for each segment one of the two previously chosen associated templates, and then generating a jittered version by moving each spike by an amount drawn from a Gaussian distribution with mean 0 and a SD 1 ms (a sample for two time segments is shown in the panel on the right hand side). Figure reproduced with permission of Häusler and Maass (2007).

450 ms and consisted of 15 consecutive time segments of length 30 ms. For each time segment 2 spike pattern templates were generated randomly. For the actual input one of the two templates of each time segment was chosen randomly (with equal probability) and a noisy variation of it was injected into the circuit, where each spike was shifted by an amount drawn from a Gaussian distribution with mean 0 and SD 1 ms. Readout neurons were trained to classify which of the two spike templates fixed for input 1 (input 2) was injected during the last time interval $[t-30\text{ ms}, t\text{ ms}]$, denoted as task $\text{tcl}_1(t)$ ($\text{tcl}_2(t)$). $\text{tcl}_1(t-\Delta t)$ ($\text{tcl}_2(t-\Delta t)$) refers to the more difficult task to classify at time $t$ the spike pattern before the last one that had been injected during the time interval $[t-60\text{ ms}, t-30\text{ ms}]$. Note that the latter task is more difficult because the relevant spike input during time $[t-60\text{ ms}, t-30\text{ ms}]$ is overwritten by new input before the readout takes place. It may be viewed as a memory task (with distractors).

Nonlinear fusion of information from both input streams was tested by training readouts to output the exclusive-or (XOR) of the two bits that represent the labels of the two templates from which the most recent spike patterns in the two input streams had been generated. Note that this computation involves a nonlinear "binding" operation on spike patterns, since it has to give a low output value if and only if the labels of the noisy spike templates injected in input streams 1 and 2 are identical. The XOR task has been used in the neural network literature as a standard example for a nonlinear computational task.

In addition we analyzed nonlinear computations on time-varying firing rates of the two input streams. The spike trains of each of the two input streams were of length 450 ms and consisted of 15 time segments of length 30 ms. For each input stream and each time segment 4 Poisson spike trains were generated with a randomly chosen time-varying frequency between 15 Hz and 25 Hz. The actual firing rates of both input streams, i.e. $r_1$ and $r_2$, used for the computations on these input firing rates, i.e. $r_1(t)/r_2(t)$ and $(r_1(t)-r_2(t))^2$, were calculated from these spike trains with a sliding window of 15 ms width. The error bars in Fig. 9 denote standard errors. All performance results are for test inputs, and freshly generated random initial conditions and random background noise for all neurons in the circuit. All simulations were carried out with the CSIM software (Natschläger et al., 2003) in combination with MATLAB. For further details see Häusler and Maass (2007).

### 2.2. Control circuits

Control circuits have the same components and the same global statistics of neurons and synaptic connections, but are missing the lamina-specific connectivity structure of data-based cortical microcircuits. Random control circuits were generated from data-based circuits by randomly rewiring recurrent synaptic connections whereas no synaptic connection was allowed to occur more than once. In order to maintain the stereotypical neuron to synapse type alignment observed for short-term synaptic plasticity (Gupta et al., 2000) the rewiring was carried out under the constraint that the pre- and post-synaptic neuron type (i.e. excitatory or inhibitory) of each synaptic connection stays the same. This constraint introduces a difference in the randomized networks generated from Thomson et al. circuits and Binzegger et al. circuits, because the numbers of synaptic connections between excitatory neurons ($N_{EE}$) are different in these two circuit templates. The same holds for the number of synaptic connections between inhibitory neurons ($N_{II}$), from inhibitory to excitatory ($N_{EI}$), and from excitatory to inhibitory neurons ($N_{IE}$), although the total number of synapses is identical for both circuits.[6] The difference is largest for $N_{II}$, which is for the Thomson et al. circuits more than three times larger. We will refer to the randomized networks generated from the two

[6] For Thomson et. al circuits (Binzegger et al. circuits) the average values of $N_{EE}$, $N_{II}$, $N_{EI}$, and $N_{IE}$ are 31,011 (32,243), 2533 (785), 5370 (4762), and 3086 (4210), respectively.

microcircuit templates as amorphous Thomson et al. and amorphous Binzegger et al. circuits.[7]

Degree-controlled circuits (Kannan et al., 1999; Maslov and Sneppen, 2002) preserve the degree distributions of neurons in all layers but otherwise lack a laminae-specific connectivity pattern. The degree of a neuron is defined as the total number of incoming and outgoing synaptic connections. Degree-controlled circuits were constructed from data-based circuits by randomly exchanging the target neurons of pairs of recurrent synaptic connections that emerge from the same neuron, and have neurons of the same type (excitatory/inhibitory) as target.

Small-world control circuits have identical cluster coefficient and average shortest path lengths as Thomson et al. circuits (but without laminae-specific synaptic connectivity pattern). They were constructed with two different algorithms, i.e. the spatial growth algorithm described in Kaiser and Hilgetag (2004) (with parameters $\alpha = 4$, $\beta = 1.32$) and the algorithm proposed by Watts and Strogatz (1998) (with parameter $\beta = 0.319$). Both algorithms were applied to generate undirected graphs that have the same size (560 nodes), clustering coefficient, and average shortest path length as Thomson et al. circuits. Each node in these graphs was replaced by a randomly drawn excitatory or inhibitory neuron (without replacement) located in one of the 6 populations of Thomson et al. circuits. Subsequently the undirected graphs were converted to directed graphs by randomly replacing each edge with a synapse (that is randomly oriented) or a reciprocal synaptic connection, with a probability so that the total number of synaptic connections and reciprocal synaptic connections is identical to the corresponding number for Thomson et al. circuits.[8]

For all control circuits the assignment of neurons to layers, the target neurons of input synapses, and the set of presynaptic neurons for hypothetical readouts was the same as for the corresponding data-based circuits.

### 2.3. Graph properties

A cortical microcircuit can be described by a directed graph with nodes (neurons) and edges (synaptic connections). A connected sub-graph with $M$ nodes is called a motif of size $M$ and has at least $M-1$ and at most $M(M-1)$ edges (ignoring self-edges). The motif count COUNT is defined as the total number of motifs of a certain type occurring in a directed graph that corresponds to a cortical microcircuit generated from a specific microcircuit template. The probability of a motif is defined as the probability that $M$ randomly drawn neurons within a microcircuit (that was randomly drawn from a specific microcircuit template) are connected according to the sub-graph defined by the motif (with no additional edges except self-edges). We analyzed sets of motifs of size $M = 2$, $M = 3$ and $M = 4$ consisting of 2, 13 and 199 sub-graphs, respectively. According to Milo et al. (2002, 2004) we did not consider motifs that contain self-edges. The motif probabilities for data-based microcircuits, amorphous circuits and degree-controlled circuits can be calculated analytically from the corresponding microcircuit templates. The templates for the connection probabilities of amorphous circuits can be obtained from data-based circuits (defined in Figs. 1 and 2) by setting the probability of each synaptic connection to the weighted average probability of all synaptic connections of the same type (defined by the type of the pre- and post-synaptic population of neurons, i.e. excitatory or inhibitory). The contribution of each synaptic connection probability to the average is weighted proportional to the product of the pre- and post-synaptic population size. The templates for the connection probabilities of degree-controlled circuits can be obtained from data-based templates by carrying out the following procedure for each type of synaptic connection. First the probability $P^s(i)$ that a randomly selected synapse of a specified type targets a specific population $i$ is calculated from the data-based template. Subsequently the probability of a synaptic connection between presynaptic population $j$ and postsynaptic population $k$ is set to the value $P^s(k)$ resulting in a connectivity pattern that is independent of the presynaptic population. Finally, the probabilities of all connections with identical presynaptic population are multiplied by a common scaling factor to obtain the same average total number of outgoing synapses for each population as for the data-based microcircuit template.

The probability of a certain motif $P^M$ is defined as the product of the probabilities for the existence or absence of each edge of a subgraph (excluding self-edges). Care has to be taken to account for permutations of neurons and different populations sizes. For a distribution of circuits consisting of $N$ neurons that were generated from a specific circuit template the mean motif count is given by

$$\overline{\mathrm{COUNT}} = \binom{N}{M} \cdot P^M$$

and the standard deviation of the motif count is defined by

$$std(\mathrm{COUNT}) = \sqrt{\binom{N}{M} \cdot P^M (P^M - 1)}$$

The motif distributions for small-world circuits were sampled using 200 circuits.

## 3. Results

### 3.1. Graph properties of the two microcircuit templates

We analyzed the two data-based cortical microcircuit templates[9] shown in Figs. 1 and 2 for their differences and similarities in connectivity structure. In order to evaluate the significance of specific structural features of the two data-based microcircuit templates we compared them with random control circuits which consist of the same number of components, i.e. neurons and synapses, but lack a laminae-specific connectivity pattern. These random control circuits were generated from data-based circuits by randomly rewiring synaptic connections.[10] This rewiring was carried out under the constraint that the pre- and post-synaptic neuron type (i.e. excitatory or inhibitory) of each synaptic connection stays the same, in order to maintain the stereotypical neuron to synapse type alignment observed for short-term synaptic plasticity Gupta et al. (2000) that we have implemented in our models. We will refer to the randomized networks generated from the two microcircuit templates as amorphous Thomson et al. and amorphous Binzegger et al. circuits.

In general the connectivity graph of Binzegger et al. circuits is more similar to the connectivity graph of the corresponding amorphous circuits than for Thomson et al. circuits. The connection probabilities defined by the laminae-specific connectivity templates (see Figs. 1 and 2) correlate with the connection probabilities of the corresponding amorphous templates with a correlation coefficient of 0.3 for Binzegger et al. circuits and 0.2 for Thomson et al. circuits.

Three graph properties have primarily been used for the characterization of naturally occurring directed graphs: clustering, degree distribution and motif distribution. A quantity often studied in

[7] Note that the connection probabilities for amorphous circuits are not uniform, but differ for each of the four synaptic connection types.

[8] It should be noted that this procedure does not reproduce the same fraction of synapse types as for data-based circuits and amorphous circuits.

[9] To be precise, each of these two templates is actually a probability distribution over graphs, rather than a specific graph.

[10] But no synaptic connection was allowed to occur more than once.

relation with clustering is the small-world property defined by Watts and Strogatz (1998). In small-world networks neighbors of a node are more likely to be neighbors themselves when compared to random graphs, thereby causing a so-called small-world effect. Nevertheless any two nodes in a small-world network are connected by a relative small number of edges, providing fast communication between any two nodes.[11] Thomson et al. circuits as well as the Binzegger et al. circuits exhibit a significant small-world property. Their cluster coefficient, that is defined as the fraction of existing edges between direct neighbors of a node, is 0.36 and 0.33, respectively, which is 37% and 30% larger than in the corresponding amorphous circuits. Both data-based microcircuit templates imply an average shortest path length of 1.77 edges, which is comparable to the average shortest path length of 1.74 edges for amorphous control circuits.

The higher cluster coefficient of Thomson et al. circuits is mainly due to excitatory and inhibitory neurons located in layer 2/3, which form highly connected hubs. The amount of convergence and divergence of a node in a graph can be specified by its degree, defined as the total number of its incoming and outgoing connections. The average degree of a layer 2/3 neuron in Thomson et al. circuits is 251, which is 20.3% larger than the average degree of 208.7 for a layer 2/3 neuron in Binzegger et al. circuits. The average degree in the remaining layers was somewhat smaller and ranged from 77.6 to 137.3 for Thomson et al. circuits and from 14.1 to 188.3 for Binzegger et al. circuits (without layer 1). Overall the average degrees of neurons in layer 2/3, 4 and 5 are correlated for both data-based circuits with a correlation coefficient of 0.74.

A third approach to characterize graphs, which also takes the direction of edges into account, is to analyze which subgraphs (motifs) occur with a frequency significantly higher or lower than in corresponding amorphous networks (see Section 2.3). The motif distributions of Thomson et al. circuits and Binzegger et al.circuits are shown in Fig. 4 for motifs consisting of two and three nodes.

The deviation of the motif distribution of the data-based microcircuits from the motif distribution of the corresponding amorphous circuits was evaluated for each motif by means of its $Z$ score (Milo et al., 2002, 2004) defined as

$$Z = \frac{\overline{\mathrm{COUNT}}_{data\text{-}based} - \overline{\mathrm{COUNT}}_{amorphous}}{std(\mathrm{COUNT}_{amorphous})},$$

where *std* denotes the standard deviation and $\overline{\mathrm{COUNT}}$ denotes the mean motif count obtained for a distribution of circuits that were generated from a specific circuit template. Remarkably the procedure of generating amorphous control circuits generates more reciprocal connections for the Thomson et al. circuits but fewer reciprocal connections for the Binzegger et al. circuits, as indicated by the $Z$ scores for motif number 2 for the motif class consisting of two nodes ($M = 2$), see Fig. 4C and E. Also the $Z$ scores for motifs consisting of three nodes differ significantly for the two templates. In particular, the motifs 3, 5 and 11 (which represent converging or diverging sub-graphs) are over-represented, whereas the motifs 2, 4 and 7 (which represent feed-forward or circular sub-graphs) are under-represented in Thomson et al. circuits. The more frequent appearance of motif 5 in Thomson et al. circuits can be attributed to the typical structure of connections from layer 4 to layer 2/3 and from layer 2/3 to layer 5. In both cases excitatory neurons within the target and the source layer are often directly synaptically connected (corresponding to the edge from the right to the top node of motif 5). Additionally, excitatory neurons in the target layer receive input from inhibitory neurons in the source layer (edge from the left to the top node of motif 5) that receive input from excitatory neurons within the source layer (edge from the right to the left node of motif 5). Therefore the excitation spreading from layer 4 (layer 2/3) to layer 2/3 (layer 5) is balanced by an inhibitory pathway passing through inhibitory neurons in layer 4 (layer 2/3).

In contrast, motifs with three nodes in Binzegger et al. circuits that consist only of two edges are significantly under-represented, whereas motifs with many edges appear more frequently than in corresponding amorphous circuits (see Fig. 4E). This may be partially attributed to the more frequent appearance of reciprocal connections compared to amorphous circuits.

The characteristic shape of the motif distribution of Binzegger et al. circuits is not due to the additional connections with layer 6, which are not specified in Thomson et al. circuits. The motif distributions of Binzegger et al. circuits with and without layer 6 have a correlation coefficient of 0.96. Moreover the characteristic shape of their motif distribution is also not caused by the comparatively high number of connections with low probability (<10%). The correlation coefficient of the motif distributions of Binzegger et al. circuits and pruned Binzegger et al. circuits, for which all connections with a connection probability lower than 10% were removed (dashed lines in Fig. 2), is 0.97.

### 3.2. Relationships between graph theoretical properties

In order to identify the structural aspects of data-based microcircuit templates that are responsible for the characteristic deviation in their motif distributions, we generated additional random control circuits which preserve the degree distributions of neurons in all layers, but otherwise lack a layer specificity of synaptic connections. These degree-controlled circuits (Kannan et al., 1999; Maslov and Sneppen, 2002) were constructed from data-based circuits by randomly exchanging the target neurons of pairs of synapses that emerge from the same neuron, and have neurons of the same type (excitatory/inhibitory) as target. In contrast to the scrambling procedure that generates amorphous circuits, this procedure preserves not only the type but also the identity of the presynaptic neuron. The motif distribution of Thomson et al. circuits changes very little through this scrambling procedure (compare Fig. 5B with Fig. 4C). The motifs 2 and 5 that represent feed-forward pathways from the right to the top node of the sub-graph (see Fig. 4A) appear less frequent, but nevertheless the $Z$ score for data-based circuits and degree-controlled circuits correlates with a correlation coefficient of 0.94. Therefore the characteristic motif distribution of Thomson et al. circuits is mainly induced by the specific distribution of degrees of neurons over layers.

In contrast, the motif distribution of degree-controlled circuits generated from Binzegger et al. circuits resembles the one for amorphous circuits (see the $Z$-score plotted in Fig. 5C). In particular, motifs consisting of many edges appear less frequently in degree-controlled circuits compared to data-based circuits. Although the $Z$ score is smaller for the majority of motifs in degree-controlled circuits, it nevertheless correlates with the $Z$ score of the Binzegger et al. circuits with a correlation coefficient of 0.79. Thus the motif distribution of Binzegger et al. circuits is induced by the laminae-specific connectivity pattern between layers and less by the specific degree distributions of neurons. Similar results are obtained for the distributions of motifs consisting of four nodes (see Fig. 6).[12]

In order to demonstrate that the motif distribution of Thomson et al. circuits cannot only be attributed to its specific clustering properties (small world property), we additionally generated control circuits with identical cluster coefficient and average shortest path

[11] Note that both properties refer to the structure of the underlying *undirected* graph, where directed edges are replaced by undirected edges.

[12] For $M = 4$ motifs the $Z$ score for Thomson et al. circuits (Binzegger et al. circuits) and the corresponding degree-controlled circuits correlates with a correlation coefficient of 0.91 (0.41).

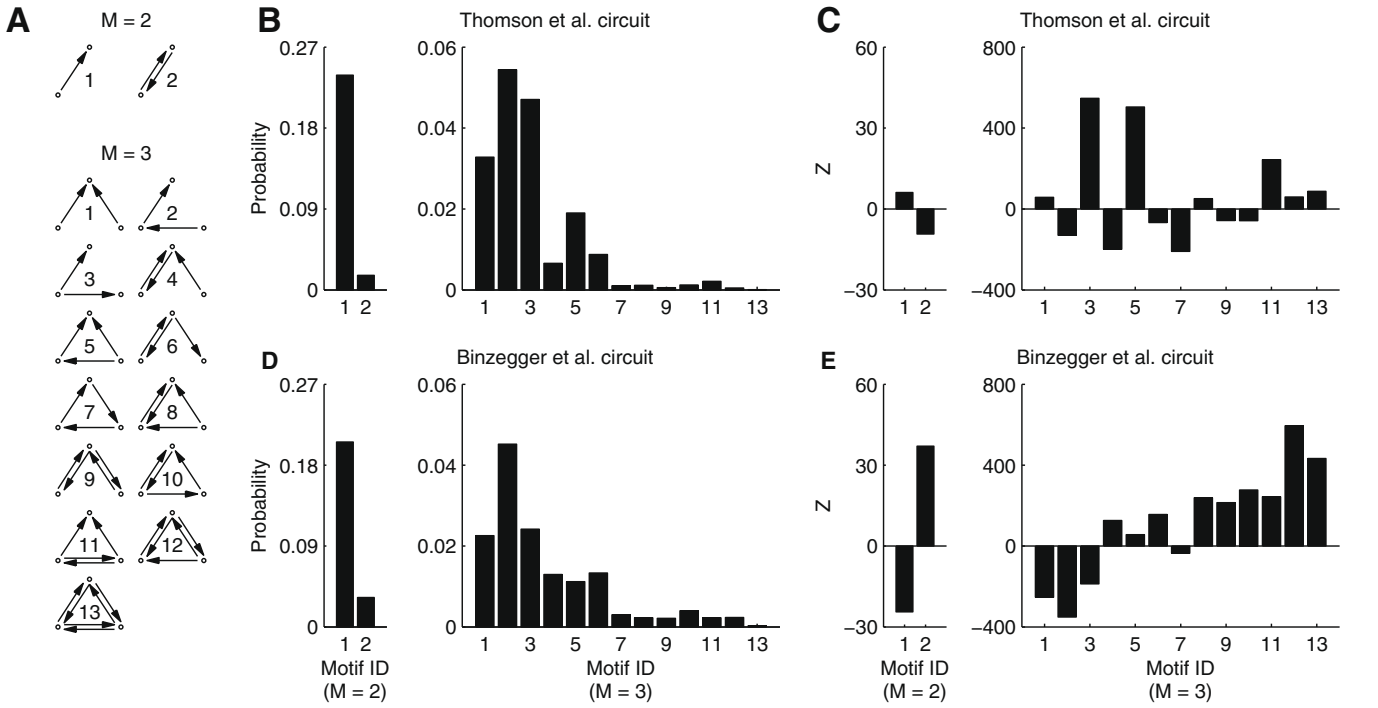


**Fig. 4.** Motif distributions for the cortical microcircuit templates of Thomson et al. (2002) (see Fig. 1) and Binzegger et al. (2004) (see Fig. 2). (A) Definition of motifs. (B) Motif probabilities for pairs (left panel) and triplets (right panel) of neurons for Thomson et al. circuits. (C) *Z* score (defined as the difference in the average motif count for the specified circuits and corresponding amorphous circuits measured in units of the standard deviation of the motif count for amorphous circuits) for pairs and triplets of neurons for Thomson et al. circuits consisting of 560 neurons and on average 42,540 synapses. (D) Motif probabilities for pairs and triplets of neurons for Binzegger et al. circuits. (E) *Z* score for Binzegger et al. circuits consisting of 560 neurons and on average 42,540 synapses. The Motif distribution for the two cortical microcircuit templates differs significantly.

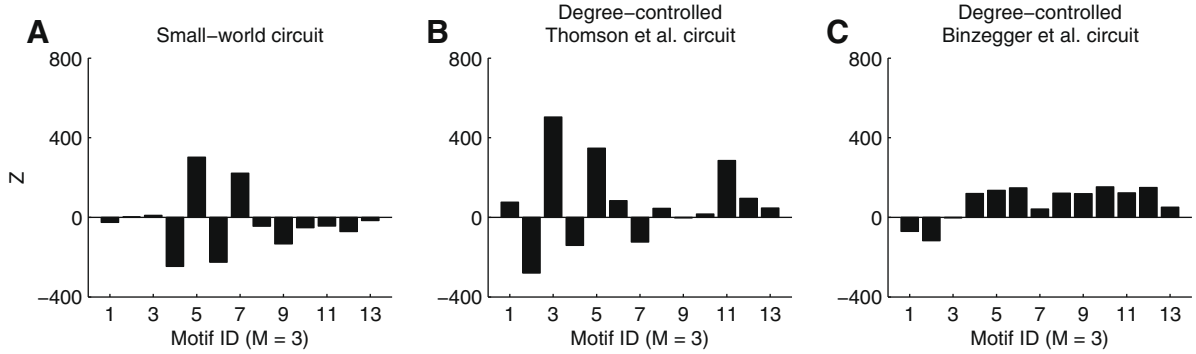


**Fig. 5.** Distributions of motifs with three nodes for three different control circuits. (A) *Z* score for small-world control circuits generated with the spatial growth algorithm described in Kaiser and Hilgetag (2004). The result for a second type of small-world control circuits generated with the algorithm proposed by Watts and Strogatz (1998) is nearly identical (correlation coefficient 0.99). (B) *Z* score for degree-controlled control circuits generated from Thomson et al. circuits. (C) *Z* score for degree-controlled control circuits generated from Binzegger et al. circuits. The degree-controlled circuits generated from Thomson et al. circuits have a *Z* score that resembles the *Z* score of Thomson et al. circuits (the average absolute difference in *Z* score represents 40% of the average absolute *Z* score for data-based circuits). In contrast, the motif distribution of degree-controlled circuits generated from Binzegger et al. circuits is more similar to the one for corresponding amorphous circuits (the average absolute difference in *Z* score is 65% of the average absolute *Z* score for data-based circuits).

length as Thomson et al. circuits but without laminae-specific synaptic connectivity pattern. In order to show that the motif distribution does not depend on a specific construction algorithm we generated two types of small-world control circuits. The first one was constructed with the spatial growth algorithm described in Kaiser and Hilgetag (2004) and the second type of control circuits was generated with the algorithm proposed by Watts and Strogatz (1998). The spatial growth algorithm of Kaiser and Hilgetag (2004) is capable of constructing networks with multiple, interconnected clusters, whereas the algorithm described by Watts and Strogatz (1998) does not preferentially connect highly connected hubs with each other. Note that both algorithms generate undirected graphs that were subsequently converted to directed graphs by randomly replacing each edge with a synapse (that is randomly oriented) or a reciprocal synaptic connection, with a probability so that the total number of synaptic connections and reciprocal synaptic connections is identical to the corresponding number for data-based circuits.[13] The $M = 3$ motif distribution for both types of small-world

[13] It should be noted that this procedure does not reproduce the same fraction of synapse types as for data-based circuits and amorphous circuits.

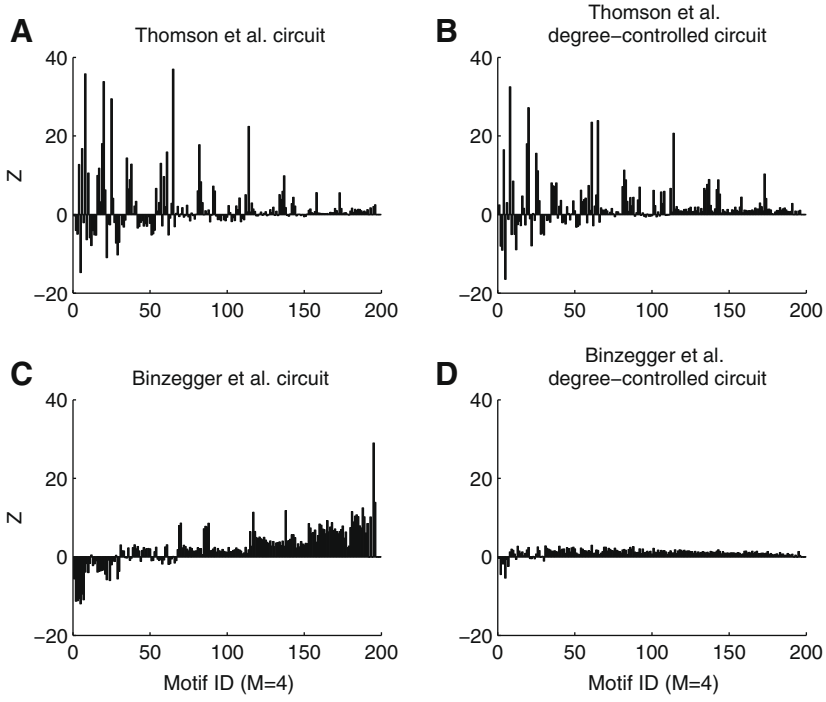


**Fig. 6.** Distributions of motifs with four nodes. (A) *Z* score for Thomson et al. circuits. (B) *Z* score for degree-controlled circuits generated from Thomson et al. circuits. (C) *Z* score for Binzegger et al. circuits. (D) *Z* score for degree-controlled circuits generated from Binzegger et al. circuits. These plots show that the degree-controlled scrambling of the connectivity structure mainly preserves the *Z* score for Thomson et al. circuits (correlation coefficient of 0.91) but not for Binzegger et al. circuits (correlation coefficient of 0.41).

circuits is similar but differs significantly from the motif distribution of data-based microcircuits (see Fig. 5A). The correlation coefficient for the motif distribution of small-world circuits, and Thomson et al. circuits and the Binzegger et al. circuits is 0.37 and −0.29, respectively.

### 3.3. Dynamical properties

We investigated the dynamical properties of Thomson et al. circuits and Binzegger et al. circuits by analyzing computer simulations of detailed cortical microcircuit models (see Section 2). Fig. 7 shows a comparison of various statistical properties of the circuit dynamics in response to generic spike inputs consisting of 40 Poisson spike trains at 20 Hz into layer 4 and layer 2/3 for both data-based circuit templates (black lines). We found that Thomson et al. circuits and Binzegger et al. circuits have very similar dynamical properties. The mean firing rate of neurons is about 24 Hz and the power spectral densities (PSD) of the mean firing rates show an excess power at low frequencies between 5 and 50 Hz. Moreover for both circuit templates the interspike interval (ISI) distributions have an exponential tail as predicted by Poisson processes. A peak in the ISI distribution around 7 ms indicates the occurrence of bursts, that is a higher probability of observing two or more spikes within a short time window of a few ms than predicted by Poisson processes with identical mean firing rates. Furthermore the distribution of the coefficient of variation of interspike intervals (CV(ISI)) of single neurons peaks at 0.72 for both circuit templates. However, the mean CV(ISI) differs significantly with a value of 0.78 (SD of 0.008) and 0.99 (SD of 0.009) for Thomson et al. circuits and Binzegger et al. circuits, respectively. As a measure of synchronous spiking activity we calculated the average cross covariance of firing rates (CC) within time bins of 1 ms for pairs of neurons (cross correlogram at time lag 0). The CC for Thomson et al. circuits and Binzegger et al. circuits is 0.035 and 0.066, respectively. Therefore, Binzegger et al. circuits operate in a more synchronous firing regime than Thomson et al. circuits.

### 3.4. Relationship between the graph structure of neural circuits and their dynamical properties

We related the dynamical properties of the data-based microcircuits to their connectivity structure by comparing the statistical properties of their circuit dynamics with the properties of corresponding control circuits (see Section 2.2).

Fig. 7 shows that degree-controlled circuits (blue lines) have similar dynamical properties when compared to corresponding data-based circuits (black lines). Only the power spectral density of degree-controlled circuits generated from Thomson et al. circuits shows a small deviation with a peak around 20 Hz. Additionally, for degree-controlled circuits generated from Binzegger et al. circuits the cross covariance of the firing rates of single neurons drops to a value of 0.05 (not shown).

In contrast, amorphous circuits have different statistical properties than data-based circuits. In particular, amorphous circuits generated from Thomson et al. circuits have a different power spectral density with a shift in power from high to low frequencies (see Fig. 7A). Furthermore the distribution of CV(ISI) differs significantly for amorphous circuits generated from Thomson et al. circuits with a higher mean CV(ISI) of 0.93 (Fig. 7E). For amorphous circuits generated from Binzegger et al. circuits the change in the CV(ISI) distribution is less pronounced with a significant drop in peak count by 7%. The mean cross covariance of the firing rates of single neurons in amorphous circuits drops significantly to a value of 0.033 and 0.045 for Thomson et al. circuits and Binzegger et al. circuits, respectively.

In order to verify that these results are in fact related to the connectivity structure and not an artifact of the specific set of scaling parameters that we had chosen for the synaptic weights of the input and the recurrent connections (see Section 2) we repeated the analysis for 40 randomly chosen scaling parameters ($S_{RW}, S_{I1}$, and $S_{I2}$) that were drawn uniformly from the interval [0.2,2] times the standard values. Subsequently we correlated the 40 values for each

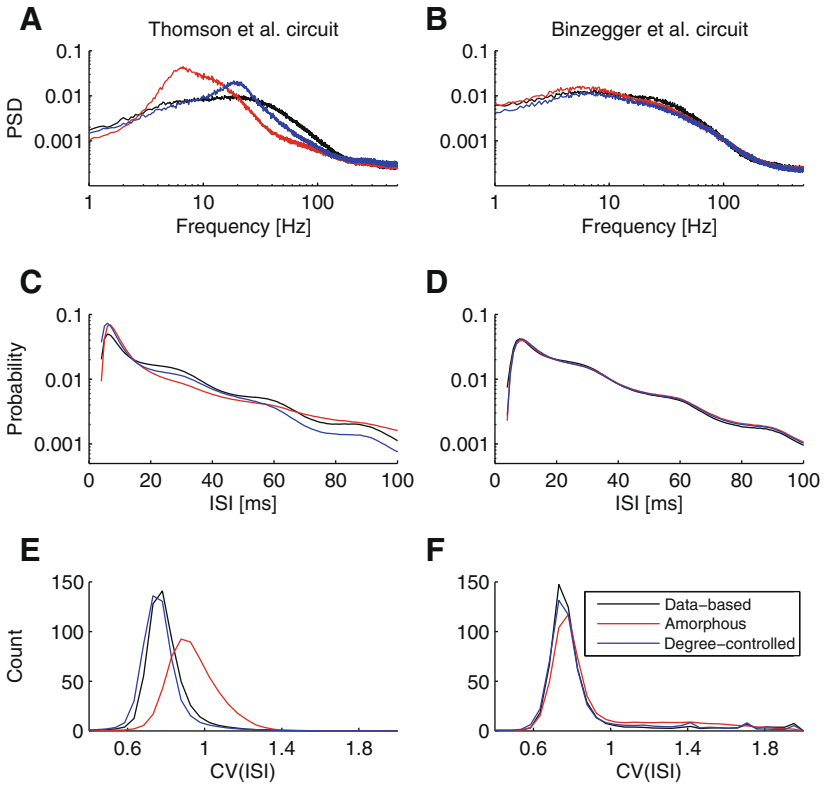


**Fig. 7.** Statistical properties of the circuit dynamics of Thomson et al. circuits (left panels) and Binzegger et al. circuits (right panels). The statistical properties of each of the two data-based microcircuits (black lines) are compared to the properties of corresponding control circuits, i.e. amorphous circuits (red lines) and degree-controlled circuits (blue lines). (A and B) Power spectral densities (PSD) of the mean firing rate (bin size 1 ms). The majority of neurons has excess power at low frequencies. (C and D) Interspike interval (ISI) distributions for different neurons. All ISI distributions are well described by exponential distributions (corresponding to straight lines in semi-log plots) predicted by Poisson processes. (E and F) Coefficient of variation of interspike intervals (CV(ISI)) for different neurons. Only for Thomson et al. circuits the corresponding amorphous circuits show different statistical properties. Error bars are negligible and omitted for clarity.

of three statistical properties for pairs of circuit types to quantify their difference in circuit dynamics. Fig. 8A illustrates the results for Thomson et al. circuits and corresponding amorphous circuits. Amorphous circuits preserve the mean firing rate of Thomson et al. circuits but change the cross covariance of the firing rates of single neurons and the coefficient of variation of ISI. In contrast, degree-controlled circuits largely preserve all three statistical properties of Thomson et al. circuits as indicated in Fig. 8B. Similar results are obtained for Binzegger et al. circuits (Fig. 8C and D).

### 3.5. Computational properties

We compared the computational properties of Thomson et al. circuits (as investigated in detail in Häusler and Maass (2007)) with the corresponding results for Binzegger et al. circuits. For this purpose we analyzed to what extent these cortical microcircuit templates support computations on information contained in generic spike inputs into layer 4 and layer 2/3, and how well they make results of these computations accessible to (hypothetical) projection neurons in layer 2/3 and layer 5. These projection neurons were modeled as linear readout neurons that were trained in a supervised manner to perform a variety of information processing tasks that are likely to be related to actual computations of cortical microcircuits.

A comparison of the performance of Thomson et al. circuits (black bars) and Binzegger et al. circuits (gray bars) for these information processing tasks is shown in Fig. 9. The performance of trained readout for test inputs (which are generated from the same distribution as the training examples, but not shown during training) was measured for all binary classification tasks by the kappa coefficient, which ranges over $[-1,1]$, and assumes a value $\geqslant 0$ if the resulting classification of test examples makes fewer errors than random guessing.[14] For tasks that require an analog output value the performance of the trained readouts was measured on test examples by its correlation coefficient with the analog target output.

It turns out that the mean performance (averaged over all tasks and readouts) for both data-based circuit models is the same, i.e. 0.50, but the performance for individual tasks differs significantly.[15] In particular for tasks involving memory or non-linear computations the performance changes heterogeneously and does not depend on the readout type or task in an obvious manner. Binzegger et al. circuits perform significantly better for the non-linear spike template classification task that involves information from both input streams during the last 30 ms (XOR task), although they have only a similar performance as Thomson et al. circuits for the classification of individual spike templates from this time segment (on which the non-linear classification is based). This suggests that Binzegger et al. circuits better support non-linear fusion of recent information from both input streams. Also the classification of earlier spike patterns in input stream 2 ($\mathrm{tcl}_2(t-\Delta t)$) is significantly better supported by these circuits. A similar effect can be observed for layer 5 readout neurons performing computations based on the firing rates of both input streams. The performance for the total task including the linear component of the computation does not differ

[14] The kappa coefficient measures the percentage of agreement between two classes expected beyond that of chance and is defined as $(P_o - P_c)/(1 - P_c)$, where $P_o$ is the observed agreement and $P_c$ is the chance agreement. Thus for classification into 2 equally often occurring classes one has $P_C = 0.5$.

[15] The performance difference for each classification tasks stays qualitatively the same for Poisson inputs at different rates (i.e. 10 Hz and 30 Hz), although the precise value of the difference and its dependence on the input firing rates differs for individual tasks and readouts.

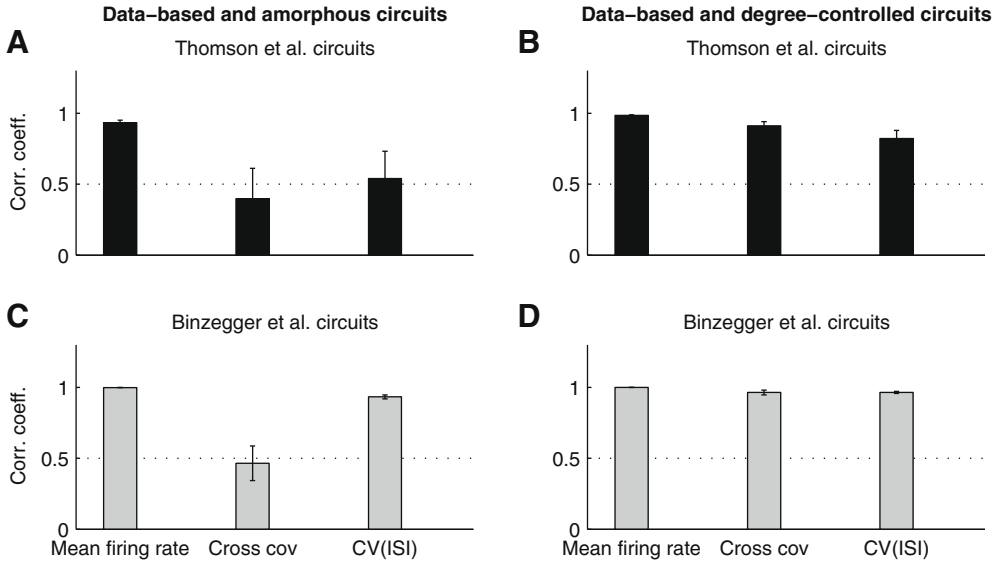


**Fig. 8.** Correlation of statistical properties of data-based circuits and corresponding control circuits for 40 randomly chosen scaling parameters for the synaptic weights of the input and the recurrent connections. Shown are correlation coefficients of the mean firing rates, the mean cross covariances of the firing rates of single neurons and the mean coefficients of variation of interspike intervals (CV(ISI)) for (A) Thomson et al. circuits and corresponding amorphous circuits, (B) Thomson et al. circuits and corresponding degree-controlled circuits, (C) Binzegger et al. circuits and corresponding amorphous circuits, and (D) Binzegger et al. circuits and corresponding degree-controlled circuits. Only degree-controlled circuits preserve the mean cross covariance and the CV(ISI) of data-based circuits. Results shown are bias corrected bootstrap estimates.

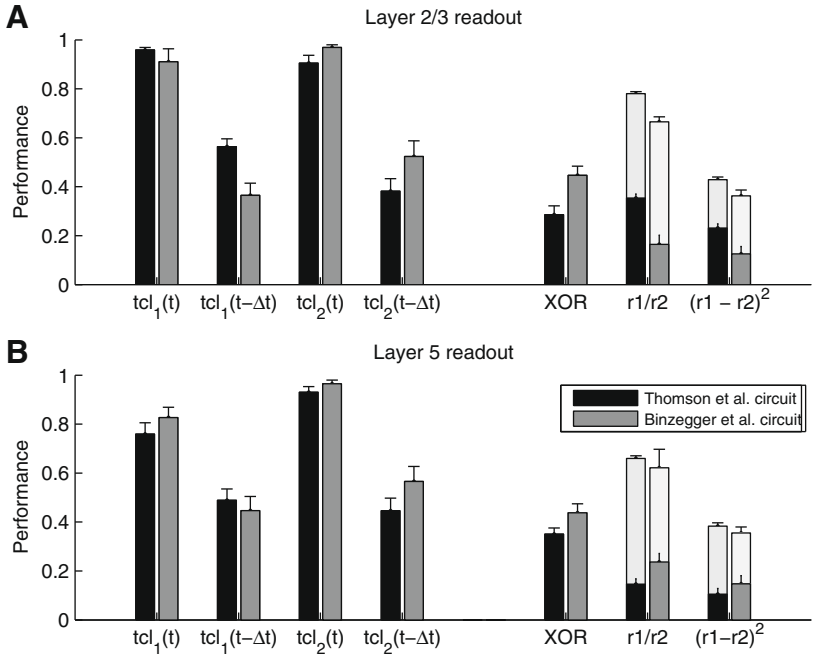


**Fig. 9.** Performance of trained linear readout neurons in layer 2/3 and layer 5 (see Section 2) for various classification tasks on spike patterns and computations performed on the rates of the two input streams for Thomson et al. circuits (black bars) and for Binzegger et al. circuits (gray bars). $\mathrm{tcl}_{1/2}(\mathrm{t})$ denotes retroactive classification of noisy spike patterns in input streams 1 or 2 that were injected during the preceding time interval [t-30 ms,t] into two classes according to the template from which each spike pattern had been generated (see Section 2 for details). $\mathrm{tcl}_{1/2}(t-\Delta t)$ refers to the more difficult task to classify at time $t$ the spike pattern before the last one that had been injected during the time interval $[t-60\ \mathrm{ms}, t-30\ \mathrm{ms}]$. For XOR classification the task is to compute at time $t = 450$ ms the XOR of the template labels (0 or 1) of both input streams injected during the preceding time segment [420 ms,450 ms]. On the right hand side the performance results for real-time computations on the time-varying firing rates $r_1(t)$ of input stream 1 and $r_2(t)$ of input stream 2 (both consisting of four Poisson spike trains with independently varying firing rates in the two input streams). The light bars show performance results for the two target functions $r_1(t)/r_2(t)$ and $(r_1(t)-r_2(t))^2$, and the bold bars for the performance on the nonlinear components of these real-time computations at any time $t$ (on the actual firing rates in both input streams during the last 30 ms). The average computational performance for both types of cortical microcircuits is similar (with a value of 0.50) but the performance for specific tasks differs significantly.

significantly, whereas the performance on the purely non-linear component is significantly better for Binzegger et al. circuits.[16]

One of the main structural features of Binzegger et al. circuits is the additional feedback loop from excitatory neurons in layer 6 to excitatory neurons in layer 4. This feedback loop turns the cortical feed-forward pathway into an intracortical closed-loop system. Remarkably, removal of this synaptic feedback doesn't significantly change the average readout performance (averaged over tasks and

[16] This non-linear component of the target functions $r1/r2$ and $(r1-r2)^2$ resulted by subtracting from these functions an (for the considered distribution of input firing rates $r1$ and $r2$) optimally fitted linear function.

readouts), but changes the performance for specific tasks. Binzegger et al. circuits without feedback perform significantly better for the two template classification tasks, i.e. classification of the previously injected spike template in input stream 1 ($\mathrm{tcl}_1(t)$) for layer 2/3 readout neurons and classification of the spike template injected before the last one in input stream 1 ($\mathrm{tcl}_1(t-\Delta t)$) for layer 5 readout neurons. On the other hand the feedback loop improves the average performance for rate tasks significantly by 25% (not shown).

### 3.6. Relationship between structure, dynamics, and computational properties of the circuits

In Häusler and Maass (2007) it was shown that the data-based laminae-specific cortical microcircuit model introduced by Thomson et al. (2002) exhibits specific computational advantages compared to various control circuits that have the same components and the same global statistics of neurons and synaptic connections, but are missing the laminae-specific connectivity pattern. In particular it was shown that degree-controlled circuits have similar average computational performance (averaged over all tasks and readouts) when compared to Thomson et al. circuits.

Here we show that the procedure of generating degree-controlled circuits, which just leaves the distribution of degrees of excitatory and inhibitory neurons in the circuit intact (as well as their roles as input-receiving node or readout-node), but randomizes their interconnectivity, does not change the computational performance of both data-based microcircuit templates in any significant manner: For Thomson et al. circuits it causes a drop by 1.6% in the average performance for the seven computational tasks, and for Binzegger et al. circuits a drop by 1.1%. Therefore the degree distribution not only preserves statistical properties of the circuit dynamics, but also computational properties for both microcircuit templates.

On the other hand it was shown in Häusler and Maass (2007) that the average performance of amorphous circuits (generated from Thomson et al. circuits), which no longer have the motif distribution of Thomson et al. circuits, drops by 25%. In contrast, for Binzegger et al. circuits the procedure of generating amorphous control circuits, which changes also for these circuits the distribution of motifs, causes a small but significant average performance improvement by 5.0%.

In order to verify that these results are general properties of the connectivity structure, and do not depend on the specific choice of the three scaling parameters $S_{I1}$, $S_{I2}$ and $S_{RW}$ for the synaptic weights of the input and the recurrent connections we repeated the analysis for 40 randomly chosen values of these scaling parameters. We obtained similar results as for our standard values of these scaling parameters: The average performance of degree-controlled circuits doesn't change significantly compared to data-based circuits with an average performance improvement by 2.6% and 0.8% for degree-controlled circuits generated from Thomson et al. circuits and Binzegger et al. circuits, respectively. In contrast, the average performance of amorphous circuits generated from Thomson et al. circuits drops significantly by 26.7% and the performance of amorphous circuits generated from Binzegger et al. circuits increases significantly by 6.0%.

That scrambling of the connectivity structure has a different effect on the average computational performance of both data-based cortical microcircuits models may be attributed to three differences in the connectivity structure of their amorphous circuits, i.e. (1) different fractions of excitatory and inhibitory synapses for both microcircuit templates, (2) a different distribution of synaptic weights for Binzegger et al. circuits (e.g. differences in synaptic strengths due to additional synaptic connections from and to layer 6 and a rescaled average synaptic weight to achieve similar firing rates for both data-based microcircuit templates) and (3) a different set of neurons within the microcircuit that is connected to the readout neurons. Note that the strengths of synaptic connection to and from layer 6 are unknown and were set to average values. Presumably a change in the strength of these connections has an effect on the computational performance of Binzegger et al. circuits.

The results for the two different microcircuit templates leave open the possibility, that specific motif distribution enhance the computational performance. But they certainly do not verify such a conjecture. To do that, one would need to be able to construct circuits with many different motif distributions. The procedure of generating degree-controlled circuits destroys the motif distribution of Binzegger et al. circuits, see Figs. 4E and 5C, but leaves the motif distribution of Thomson et al. circuits largely unchanged (Figs. 4C and 5B). It also changes the number of reciprocal connections, because the magnitude of the $Z$ score of the second $M = 2$ motif drops consistently by 56% and 38% for Thomson et al. circuits and Binzegger et al. circuits, respectively. These results show that there are cases where the motif distribution changes significantly, but the computational performance remains largely the same.

In order to investigate whether the computational properties can be in fact related to specific dynamical properties that are preserved by degree-controlled circuits we correlated three statistical measures for circuit dynamics with the average computational performance (averaged over all tasks and readouts) for 40 randomly chosen values of the scaling parameters for the synaptic weights of the input and the recurrent connections. Fig. 10 shows that the mean coefficient of variation of ISIs and the mean cross covariance of the firing rate of single neurons correlate with the average computational performance for Thomson et al. circuits and Binzegger et al. circuits (although with a somewhat smaller value for the correlation coefficient between performance and mean cross covariance of the firing rates). Therefore, for the set of computational tasks considered in this article the best performance is achieved in the regular asynchronous firing regime with small values for the mean cross covariance and the mean coefficient of variation of ISIs. For both data-based microcircuit models the mean firing is positively correlated with the average performance.

## 4. Discussion

We found that (1) the microcircuit template by Binzegger et al. (2004) and the microcircuit template by Thomson et al. (2002) have significant small-world properties, but quite different motif distributions; (2) both data-based microcircuits have similar circuit dynamics and average computational capabilities but different computational properties for individual tasks; and (3) the degree distribution is the aspect of the connectivity structure of both data-based microcircuit templates that is responsible for their dynamical properties and their computational properties.

### 4.1. Similar global structural properties but different motif distributions

Thomson et al. circuits and Binzegger et al. circuits have similar small-world properties and their degree-distributions share characteristic main features. For both circuit templates the average degree was highest for excitatory neurons in layer 2/3, suggesting the importance of hubs in a layer where both cortical input streams merge. Furthermore the average degree of neurons in layer 2/3, layer 4 and layer 5 correlates for both cortical microcircuit templates (correlation coefficient of 0.74).

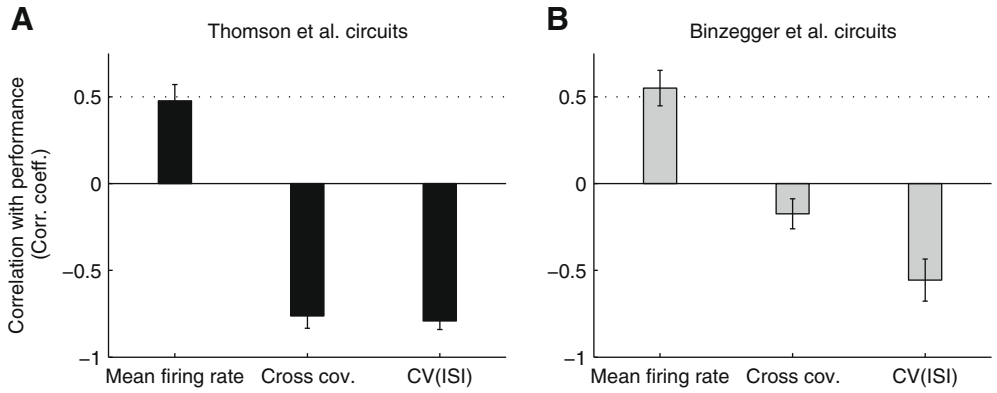


**Fig. 10.** Correlation of the mean computational performance (averaged over all tasks and readouts in Fig. 9) and three statistical properties of the circuit dynamics for 40 randomly chosen scaling parameters for the synaptic weights of the input and the recurrent connections. (**A**) Results for Thomson et al. circuits. (**B**) Results for Binzegger et al. circuits. These results suggest that the best performance is achieved in the regular asynchronous firing regime. Results shown are bias corrected bootstrap estimates.

The somewhat more amorphous-like connectivity pattern of Binzegger et al. circuits may be attributed to a few diffuse synaptic connections that are emerging at the boundaries between two adjacent layers. These might be the results of slightly shifted layer boundaries for several three-dimensional cell reconstructions obtained at different locations in the primary visual cortex. Dendritic and axonal arbors of two cells, which are non-overlapping in case of precise layer boundaries, could in case of shifted layer-boundaries account for additional diffuse synaptic connectivity.

The most distinct structural difference between the two microcircuit templates is expressed in their motif distribution (Figs. 4 and 6).[17]

The number of reciprocal connections for Thomson et al. circuits is smaller than for the corresponding amorphous circuits (Fig. 4C), whereas for the Binzegger et al. circuits it is twice as large as for amorphous circuits (Fig. 4D). Furthermore only for Binzegger et al. circuits highly connected motifs consisting of three nodes are over-represented (Fig. 4E), whereas the motif distribution for Thomson et al. circuits (Fig. 4C) can be primarily attributed to their degree-distribution. Scrambling the connectivity structure while leaving the degrees of nodes invariant does not change the motif distribution for Thomson et al. circuits (see Figs. 5 and 6) but for Binzegger et al. circuits.

Remarkably, the motif distribution of Thomson et al. circuits matches to some degree the motif distribution of a superfamily of biological information-processing networks reported in Milo et al. (2004). Their connectivity patterns show highly over-represented three node motifs 5, 8, and 11 and are lacking motifs 1, 3, 4, and 6 when compared to random networks. Analogous, in Thomson et al. circuits motifs 5 and 11 occur with a frequency significantly higher than in random networks, whereas motif 4 is under-represented. The feedforward motif 5 has been theoretically and experimentally linked to signal-processing tasks such as persistence detection and pulse generation (see Alon, 2006). However, the frequent occurrence of motif 3 is atypical for this superfamily.

It should be noted that the different results for Thomson et al. circuits and Binzegger et al. circuits are not contradictory but rather point out structural differences between potential synaptic connectivity specified by Binzegger et al. circuits and functional synaptic connectivity specified by Thomson et al. circuits. In principle Thomson et al. circuits can be considered as sub-graphs of Binzegger et al. circuits which were shaped by synaptic plasticity according to their specific functional role. Furthermore the number of synapses in a microcircuit has an effect on the local and global structural properties. We introduced for each cortical microcircuit template to some extent arbitrarily a global constant factor that scales all synaptic connection probabilities to match the average total number of synaptic connections for Thomson et al. circuits and Binzegger et al. circuits.

### *4.2. Similar circuit dynamics and average computational capabilities but different computational properties*

Both microcircuit templates have similar circuit dynamics (Fig. 7). The power spectral densities show an excess power at low frequencies between 5 and 50 Hz, which is consistent with experimental results showing peaks in the 20–60 Hz range for cells in area MT in behaving Monkey (Bair et al., 1994). The interspike interval distributions show no evidence for power-law behavior but have exponential tails as predicted by Poisson processes. Neurons slightly tend to burst with longer periods of low firing activity resembling experimental results obtained in cat cerebral cortex during slow wave sleep (Bedard et al., 2006; Destexhe et al., 1999; Steriade, 2003). The most frequently occurring value of the coefficient of variation of interspike intervals for neurons in the circuits that we considered was for both microcircuit templates 0.72. This value is lower than the reported value of about 1 for MT cells and V1 cells in behaving monkey (Softky and Koch, 1992, 1993) in response to bars and textured stimuli. This might be attributed to a missing diversity in neuron types (e.g. bursting and stuttering cells), synapse types (e.g. NMDA receptors), and a missing calcium dynamics that introduces processes on many different time scales.

It turned out that the average information processing capabilities of Thomson et al. circuits and Binzegger et al. circuits are similar but differ for specific tasks (Fig. 9). In particular for the chosen set of seven computational tasks Binzegger et al. circuits support slightly superior non-linear fusion of information contained in both input streams.

The degree distribution is the aspect of the connectivity structure of both data-based microcircuit templates that is responsible for their dynamical properties and their computational properties

### *4.3. The degree distribution determines the dynamical properties and the computational properties*

The degree distribution of neurons largely determines the circuit dynamics for both microcircuit templates. Degree-controlled circuits largely preserve the mean cross covariances of the firing

[17] The motif distributions for both data-based cortical microcircuits differ significantly from the motif distributions of corresponding amorphous circuits that were generated from the two data-based cortical microcircuits by scrambling their connectivity structure, but these differences are not consistent for both data-based cortical microcircuits.

rates of neurons and the mean coefficients of variation of interspike intervals of data-based circuits independent of the dynamic regime controlled by the scaling parameters for the synaptic weights of the input and the recurrent connections (Fig. 8).

When we changed the connectivity structure of these two microcircuit models in order to see which aspects of it are essential for the computational performance, we found in agreement with Häusler and Maass (2007) that the distribution of degrees of nodes is also a key factor for their computational performance. Scrambling the connectivity structure but leaving the degree distribution of neurons invariant did not result in a change in the average computational performance (see Section 3.6).

These results suggest that the degree-controlled scrambling of the connectivity structure preserves specific statistical properties of the circuit dynamics that are crucial for information processing and correlate with the average computational performance (Fig. 10). For the chosen set of information processing tasks the best performance is achieved in the regular asynchronous firing regime.

It is interesting to relate these results to theoretical results obtained for much simpler models. Ganguli et al. (2008) showed for networks consisting of linear neurons that the graph structure has an impact on the computational properties, more precisely the memory capacity of the network. Furthermore, Schrauwen et al. (2009) have shown by means of mean-field analysis that the performance of randomly connected recurrent networks built from neurons whose output can only take one of two values (binary output) depends strongly on the network connectivity structure and is related to the in-degree of neurons in addition to the distribution of synaptic weights.

It can be verified by amorphous control circuits that scrambling of the connectivity structure can have different effects on the average computational performance. Such scrambling increases the average performance for Binzegger et al. circuits but decreases the average performance for Thomson et. al circuits. This suggests that only Thomson et al. circuits are optimized for a specific set of computations, whereas Binzegger et al. circuits represent potential synaptic connections that provide the possibility of implementing various different sets of computations.

#### *4.3.1. Suggestions for further experimental and simulation based research*

The results of this article point to three directions for further research. First, further work is needed to provide more reliable microcircuit models. The two data-based cortical microcircuit templates were estimated with different experimental techniques, i.e. dual intracellular recordings in vitro and three-dimensional cell reconstructions, and it is up to now unclear how to relate them to each other or if possible merge them to one unified cortical microcircuit template. Both microcircuit templates do not account for the lateral connectivity patterns of the neocortex. The Thomson et al. microcircuit template was estimated from neurons in slices within a maximum horizontal distance of 100 μm, whereas the Binzegger et al. microcircuit template was obtained by averaging statistical data of whole cell reconstructions discarding information about horizontal locations of neurons. Current work in progress Potjans and Diesmann (2008) suggests that the assumption of Gaussian lateral connectivity patterns presumably explains to some extent the discrepancies between both microcircuit templates. Merging both datasets could potentially result in a unified microcircuit template with computational properties and circuit dynamics in between those obtained for the two microcircuit templates analyzed in this study.

Secondly, a thorough empirical analysis of the distribution of motifs (especially for more than two nodes) in cortical microcircuits is needed. So far we can only analyze the distribution of motifs that is induced by data connection probabilities for any two neurons $A$ and $B$. Preliminary data suggest however, that the probability of a synaptic connection from $B$ to $A$ depends on the presence of a synaptic connection from $A$ to $B$. For instance whole-cell recordings of layer 5 pyramidal neurons of somatosensory, visual and prefrontal areas have shown that reciprocal connections are $\geqslant 3$ times more likely than in random networks (Holmgren et al., 2003; Markram, 1997; Song et al., 2005; Wang et al., 2006). Similarly for three neurons $A$, $B$, $C$ (of specific types) the probability of a synaptic connection from $C$ to $A$ is likely to depend on the presence or absence of other synaptic connections between $A$, $B$, $C$. This was confirmed by triple and quadruple whole-cell recordings of layer 5 pyramidal neurons in the rat visual cortex that showed that motifs consisting of many edges are over-represented when compared to random networks (Song et al., 2005). Likewise the probability that a layer 2/3 pyramidal neuron in rat somatosensory cortex makes a synaptic connection with two layer 5 neurons is fourfold higher compared with random connectivity if the layer 5 neurons are synaptically connected (motif 5 and 8) (Kampa et al., 2006). In contrast the probability that a layer 5 pyramidal neuron receives input from two layer 2/3 pyramidal neurons is threefold higher compared with random networks if the layer 2/3 pyramidal neurons are not connected (motif 1). Reliable data for such conditioned connection probabilities are needed not only for all possible types of neurons $A$, $B$, $C$, but also for all possible laminar locations of these three neurons.

Finally, the microcircuit templates should be tested on a larger variety of computational tasks. Our results on the computational performance of the two microcircuit templates and several variations of them depend on a somewhat arbitrary choice of seven concrete computational tasks, and on the decision to only specialize the synaptic weights of readout neurons for a specific computational task, while having the weights within the circuit chosen from data-based probability distributions(hence not specialized for a particular computational task). Furthermore the results presumably depend also on the specific choice of distributions for input spike trains from external sources. In particular, geniculate relay cells have a firing pattern that can vary between tonic and bursting (Sherman, 1996). Burst firing has been shown to make a strong contribution to the initial phasic part of visual responses to gratings (Guido et al., 1992) and flashed spots (Guido and Sherman, 1998).

## 5. Conclusions

This article has shown that the two available templates for cortical microcircuits have quite interesting structural, dynamical, and computational features. In particular we have shown that it is possible to relate the structure and the (conjectured) computational function of these two microcircuit templates. This positive result will hopefully stimulate further systematic experimental work on the anatomy and physiology of cortical microcircuits, that is needed in order to arrive at a definite understanding of the computational function of cortical microcircuits and their genetically encoded structural basis.

## Acknowledgements

We would like to thank Tom Binzegger, Rolf Kötter, Henry Markram, Olaf Sporns, and Alex Thomson for helpful discussions on research related to this article. We also would like to thank two anonymous referees for helpful comments.

## References

Alon, U., 2006. An Introduction to Systems Biology: Design Principles of Biological Circuits. Chapman & Hall/CRC, Boca Raton, US.

Bair, W., Koch, C., Newsome, W., Britten, K., 1994. Power spectrum analysis of bursting cells in area MT in the behaving monkey. J. Neurosci. 14 (5 Pt 1), 2870–2892.

Bedard, C., Kroger, H., Destexhe, A., 2006. Does the 1/*f* frequency scaling of brain signals reflect self-organized critical states? Phys. Rev. Lett. 97 (11), 118102.

Binzegger, T., Douglas, R.J., Martin, K.A., 2004. A quantitative map of the circuit of cat primary visual cortex. J. Neurosci. 24 (39), 8441–8453.

Callaway, E.M., 2004. Feedforward, feedback and inhibitory connections in primate visual cortex. Neural Networks 17 (5–6), 625–632.

Dantzker, J.L., Callaway, E.M., 2000. Laminar sources of synaptic input to cortical inhibitory interneurons and pyramidal neurons. Nature Neurosci. 3 (7), 701–707.

Destexhe, A., Contreras, D., Steriade, M., 1999. Spatiotemporal analysis of local field potentials and unit discharges in cat cerebral cortex during natural wake and sleep states. J. Neurosci. 19 (11), 4595–4608.

Destexhe, A., Rudolph, M., Fellous, J.M., Sejnowski, T.J., 2001. Fluctuating synaptic conductances recreate in vivo-like activity in neocortical neurons. Neuroscience 107 (1), 13–24.

Douglas, R.J., Koch, C., Mahowald, M., Martin, K., Suarez, H., 1995. Recurrent excitation in neocortical circuits. Science 269 (5226), 981–985.

Douglas, R.J., Martin, K.A., 2004. Neuronal circuits of the neocortex. Annu. Rev. Neurosci. 27, 419–451.

Ganguli, S., Huh, D., Sompolinsky, H., 2008. Memory traces in dynamical systems. PNAS USA 105, 18970–18975.

Guido, W., Lu, S.M., Sherman, S.M., 1992. Relative contributions of burst and tonic responses to the receptive field properties of lateral geniculate neurones in the cat. J. Neurophysiol. 68, 21992211.

Guido, W., Sherman, S.M., 1998. Response latencies of cells in the cats lateral geniculate neurones are less variable during burst than tonic firing. Visual Neurosci. 15, 231237.

Gupta, A., Wang, Y., Markram, H., 2000. Organizing principles for a diversity of GABAergic interneurons and synapses in the neocortex. Science 287, 273–278.

Häusler, S., Maass, W., 2007. A statistical analysis of information processing properties of lamina-specific cortical microcircuit models. Cerebral Cortex 17 (1), 149–162.

Holmgren, C., Harkany, T., Svennenfors, B., Zilberter, Y., 2003. Pyramidal cell communication within local networks in layer 2/3 of rat neocortex. J. Physiol. 551 (Pt 1), 139–153.

Kaiser, M., Hilgetag, C., 2004. Spatial growth of real-world networks. Phys. Rev. E 69, 036103.

Kalisman, N., Silberberg, G., Markram, H., 2005. The neocortical microcircuit as a tabula rasa. Proc. Natl. Acad. Sci. 102 (3), 880–885.

Kampa, B.M., Letzkus, J.J., Stuart, G.J., 2006. Cortical feed-forward networks for binding different streams of sensory information. Nature Neurosci. 9 (12), 1472–1473.

Kannan, R., Tetali, P., Vempala, S., 1999. Simple Markov-chain algorithms for generating bipartite graphs and tournaments. Random Struct. Algorithms 14 (4), 208–293.

Maass, W., Natschläger, T., Markram, H., 2002. Real-time computing without stable states: a new framework for neural computation based on perturbations. Neural Comput. 14 (11), 2531–2560.

Markram, H., 1997. A network of tufted layer 5 pyramidal neurons. Cerebral Cortex 7, 523–533.

Markram, H., Wang, Y., Tsodyks, M., 1998. Differential signaling via the same axon of neocortical pyramidal neurons. PNAS 95, 5323–5328.

Maslov, S., Sneppen, K., 2002. Specificity and stability in topology of protein networks. Science 296 (5569), 910–913.

Milo, R., Itzkovitz, S., Kashtan, N., Levitt, R., Shen-Orr, S., Ayzenshtat, I., Sheffer, M., Alon, U., 2004. Superfamilies of evolved and designed networks. Science 303 (5663), 1538–1542.

Milo, R., Shen-Orr, S., Itzkovitz, S., Kashtan, N., Chklovskii, D., Alon, U., 2002. Network motifs: simple building blocks of complex networks. Science 298 (5594), 824–827.

Mountcastle, V.B., 1998. Perceptual Neuroscience: The Cerebral Cortex. Harvard University Press, Cambridge.

Natschläger, T., Markram, H., Maass, W., 2003. Computer models and analysis tools for neural microcircuits. In: Kötter, R. (Ed.), Neuroscience Databases. A Practical Guide. Kluwer Academic Publishers, Boston, pp. 123–138 (chapter 9).

Nelson, S., 2002. Cortical microcircuits: diverse or canonical? Neuron 36 (1), 19–27.

Newman, M.E., 2003. The structure and function of complex networks. SIAM Rev. 45, 167–256.

Potjans, T.C., Diesmann, M., 2008. Integration of anatomical and physiological connectivity data sets for layered cortical network models. Seventeenth Annual Computational Neuroscience Meeting: CNS*2008, July 19–24th 2008, Portland, Oregon, USA. BMC Neuroscience 2008, 9(Suppl. 1)(P60).

Schrauwen, B., Büsing, L., Legenstein, R., 2009. On computational power and the order-chaos phase transition in reservoir computing. Proceeding of NIPS 2008, Advances in Neural Information Processing Systems, vol. 21. MIT Press, pp. 1425–1432.

Shen-Orr, S.S., Milo, R., Mangan, S., Alon, U., 2002. Network motifs in the transcriptional regulation network of escherichia coli. Nat. Genet. 31, 64–68.

Sherman, S.M., 1996. Dual response modes in lateral geniculate nucleus: mechanisms and function. Visual Neurosci. 13, 205213.

Silberberg, G., Gupta, A., Markram, H., 2002. Stereotypy in neocortical microcircuits. Trends Neurosci. 25 (5), 227–230.

Softky, W.R., Koch, C., 1992. Cortical cells should fire regularly, but do not. Neural Comput. 4 (5), 643–646.

Softky, W.R., Koch, C., 1993. The highly irregular firing of cortical cells is inconsistent with temporal integration of random EPSPs. J. Neurosci. 13 (1), 334–350.

Song, S., Sjostrom, P.J., Reigl, M., Nelson, S., Chklovskii, D.B., 2005. Highly nonrandom features of synaptic connectivity in local cortical circuits. PLoS Biol. 3 (3), e68.

Steriade, M., 2003. Neuronal Substrates of Sleep and Epilepsy. Cambridge University Press, Cambridge, UK.

Strogatz, S.H., 2001. Exploring complex networks. Nature 410, 268–276.

Thomson, A.M., 2005. Personal communication.

Thomson, A.M., Lamy, C., 2007. Functional maps of neocortical local circuitry. Front. Neurosci. 1 (1), 19–42.

Thomson, A.M., West, D.C., Wang, Y., Bannister, A.P., 2002. Synaptic connections and small circuits involving excitatory and inhibitory neurons in layers 2–5 of adult rat and cat neocortex: triple intracellular recordings and biocytin labelling in vitro. Cerebral Cortex 12 (9), 936–953.

Wang, Y., Markram, H., Goodman, P.H., Berger, T.K., Ma, J., Goldman-Rakic, P.S., 2006. Heterogeneity in the pyramidal network of the medial prefrontal cortex. Nat. Neurosci. 9 (4), 534–542.

Watts, D.J., Strogatz, S.H., 1998. Collective dynamics of 'small-world' networks. Nature 393, 440–442.

White, E.L., 1989. Cortical Circuits. Birkhaeuser, Boston.